PHYSICAL REVIEW B VOLUME 56, NUMBER 10 1 SEPTEMBER 1997-II

Perpendicular magnetic anisotropy of the epitaxial fcc Co/60-Å-Ni/Cu(001) system

Jaeyong Lee, G. Lauhoff, and J. A. C. Bland
Cavendish Laboratory, University of Cambridge, Madingley Road, Cambridge CB3 0HE, United Kingdom

(Received 29 May 1997; revised manuscript received 1 July 1997)

We have studied the transition from perpendicular to in-plane magnetization in a ferromagnetically coupled epitaxial Co/Ni/Cu(001) structure. Perpendicular magnetic anisotropy (PMA) up to 6 ± 1.5 Å Co thickness is observed. The value of the uniaxial Co volume anisotropy (K_V^{Co}), which comes entirely from the shape anisotropy contribution, is explained by the absence of strain in the Co film, leading to a vanishing magnetoelastic anisotropy contribution to K_V^{Co} as evidenced by reflection high-energy electron diffraction results. We conclude that the critical thickness for PMA in this system can be controlled via strain in the Co film. [S0163-1829(97)50734-X]

The phenomenological explanation for the occurrence of perpendicular magnetic anisotropy[1] (PMA) in ultrathin films is the competition of the volume anisotropy which favors an in-plane easy axis and the symmetry breaking surface/interface anisotropy[2] which favors PMA. Studies of PMA have mainly used magnetic films grown on a nonmagnetic metal[3,4] and multilayers with nonmagnetic spacers[5,6] in order to increase the surface/interface effects. Multilayers in which both types of layers are ferromagnetic (FM) have not been a popular choice because the interface anisotropy has to overcome an additional shape anisotropy, namely that of the second ferromagnetic layer. The PMA of fcc [111] textured Co/Ni multilayers is one of the exceptions to the above argument and is explained by the contribution of the interface between ultrathin closed-packed layers.[7] Another example of PMA shown in FM/FM layers has been reported for fcc/fct metastable Fe/15 ML Ni/Cu(001) structures.[8] Until now the engineering of PMA has mainly concentrated on finding symmetry breaking surface/interface anisotropies by using different combinations of film and substrate. However little attention has been paid to extending the critical thickness (t_c^{PMA}) for PMA, which is another important factor for technical applications. Therefore while an epitaxial Cu/25 Å Ni/Cu(001) structure shows PMA, epitaxial Cu/Ni (17 Å)/Co (2–10 Å)/Ni (8 Å)/Cu(001) structures did not show PMA although the interface anisotropy ($K_S^{\mathrm{Co/Ni}}$) of Co and Ni was found to prefer PMA and 2 Å Co was inferred as the value for t_c^{PMA}.[9] This finding was explained to result from an extraordinarily large Co volume anisotropy (K_V^{Co}), associated with a magnetoelastic anisotropy due to strain.

The present work is based on the recognition that t_c^{PMA} in the Ni/Co system can be extended by decreasing the absolute value of K_V^{Co}. This can be realized by minimizing the lattice misfit between fcc Co and Ni. The in-plane lattice parameter of Ni can in principle be controlled continuously by growing the Ni film on Cu(001) beyond the coherent growth region. In this paper we report our observation of the PMA of an fcc Cu/Co step-wedge/60 Å Ni/1000 Å Cu/Si(001) structure. Our findings suggest a way of controlling t_c^{PMA} in this system by controlling the strain in the magnetic film.

The Si(001) substrate was etched in diluted HF solution for 12 minutes prior to loading into the growth chamber and annealed for 2 hours at $\sim 200\,°\mathrm{C}$ after overnight bake-out. The base pressure of the chamber was 6×10^{-10} mbar and during deposition increased to 3×10^{-9} mbar. Cu buffer layers were grown at ~ 15 Å/min using an electron beam heated Mo crucible while Co and Ni films were grown at $1\sim1.5$ Å/min by electron beam evaporation. A 60 Å Ni/1000 Å Cu buffer was prepared on the Si(001) substrate and a step-wedged ($0\sim27$ Å) Co epitaxial film was grown on it. A 30-Å Cu capping layer was further deposited for *ex situ* measurements. The film thickness was estimated using a quartz crystal monitor close to the sample position. The cleanliness of the film was confirmed by Auger electron spectroscopy after completion of each film growth.

The reflection high energy electron diffraction (RHEED) images were taken with a CCD camera during film growth. RHEED patterns confirmed the earlier finding[10] that three-dimensional epitaxial growth occurs along the [001] direction with the Cu and Ni cubic axes rotated in-plane by 45° with respect to the Si(001) principal axes. Figure 1 shows a typical RHEED picture taken after the completion of the growth of the corresponding layer along two different Cu azimuths. After 1000 Å Cu deposition, sharp streaks with low background were observed in the RHEED pattern. No qualitative change of the RHEED pattern was observed during the subsequent Ni and Co growth, revealing that the structure of an overlying Co film has an fcc structure and the same cubic axis direction as in Cu and Ni. This epitaxial relationship between Co and Ni is expected because the lattice mismatch between fcc Ni and fcc Co is very small ($a_0=3.56$ Å for the fcc Co phase and $a_0=3.52$ Å for fcc Ni) and both films have an fcc (001) surface when grown on Cu(001).[10,11]

Figure 2 shows magneto optic Kerr effect (MOKE) hysteresis loops with varying Co thickness. In the polar MOKE measurements the light was incident at 90° to the surface and for the longitudinal MOKE it was at 45° to the surface and along the ⟨100⟩ Ni azimuth. The MOKE loops of a 60 Å Ni/Cu(001) ($t^{\mathrm{Co}}=0$ Å) show PMA as reported by other groups.[10,12] It is clear that the easy axis of this system is perpendicular to the surface up to 4 Å Co thickness and in the plane at 8 Å Co thickness. The in-plane MOKE loops with 0 and 4 Å Co overlayers show strong hysteresis behav-

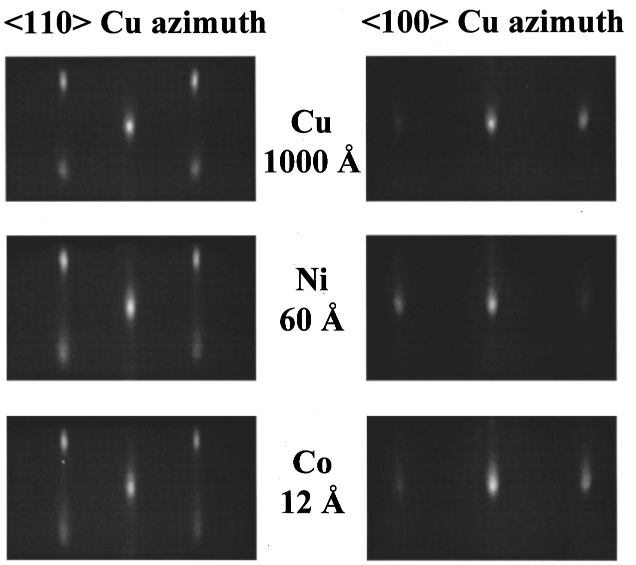

FIG. 1. RHEED images of 1000 Å Cu/Si(001), 60 Å Ni/1000 Å Cu/Si(001), and 12 Å Co/1000 Å Cu/Si(001). Qualitatively, there is not much difference, confirming the epitaxial relationship among them.

ior. This hysteresis is due to the sensitivity of the longitudinal MOKE geometry to the perpendicular component of the magnetization. As the magnetic field decreases from saturation, the magnetization starts to rotate towards the easy axis which is the surface normal. Therefore, the perpendicular component of magnetization is also recorded in the longitudinal geometry.

The magnetic anisotropy was determined using polar MOKE measurements for the Co thickness range where the magnetization was in the plane. We assume that the Co and Ni are very strongly ferromagnetically coupled, i.e., the coupling strength is much larger than all relevant anisotropy

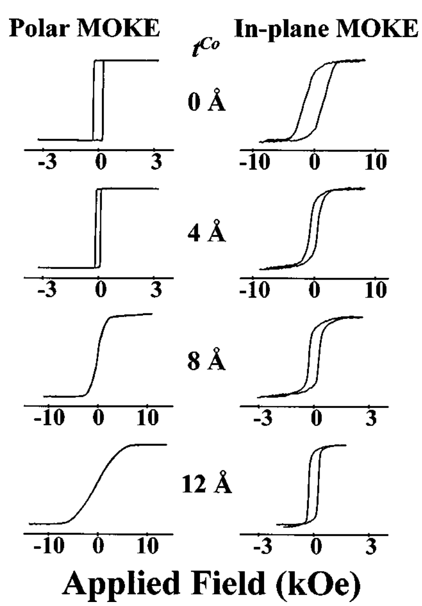

FIG. 2. Polar MOKE (left) and in-plane MOKE along ⟨10⟩ direction (right) loops for different Co thicknesses. The magnetic field ranges (x axis) are different for each geometry depending on the direction of the easy axis of magnetization.

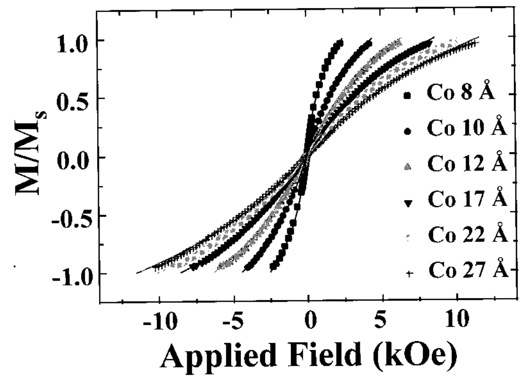

FIG. 3. Normalized polar M-H curves and fitted curves [see text including Eq. (3)].

fields. We follow a phenomenological model, in which the second-order magnetic anisotropy constant (K_1) of the whole structure is described as

$$K_1 D = K_V^{\mathrm{Co}} t^{\mathrm{Co}} + 2K_S^*, \tag{1}$$

where

$$2K_S^* = K_S^{\mathrm{Co/Ni}} + K_S^{\mathrm{Ni/Cu}} + K_S^{\mathrm{Co/Cu}} + K_V^{\mathrm{Ni}} t^{\mathrm{Ni}} \tag{2}$$

and D, t^{Co}, and t^{Ni} are the total thickness of magnetic films ($D = t^{\mathrm{Co}} + t^{\mathrm{Ni}}$), Co thickness, and Ni thickness, respectively. A similar expression arises for the fourth-order anisotropy constant (K_2). But the effective magnetic anisotropy constant of the whole structure (K_{eff}) has contributions from both the second-order and fourth-order cubic anisotropy constants. The strong curvature of the polar loop at 8 and 12 Å in the polar geometry of Fig. 2 suggests that K_2 is not negligible compared to K_1 and from the loop shape we infer that the K_2 contribution is more important in the 8 Å Co than in the 12 Å Co film. The out-of-plane M-H relation for films with in-plane easy axis is

$$H = -\frac{2K_1}{M_S}\left(\frac{M}{M_S}\right) - \frac{4K_2}{M_S}\left(\frac{M}{M_S}\right)^3, \tag{3}$$

where the saturation field is obtained when $M = M_S$ and the effective magnetization (M_S) of this system is given by

$$M_S = \frac{M_S^{\mathrm{Co}} t^{\mathrm{Co}} + M_S^{\mathrm{Ni}} t^{\mathrm{Ni}}}{t^{\mathrm{Co}} + t^{\mathrm{Ni}}}, \tag{4}$$

where M_S^{Co} and M_S^{Ni} are assumed to be the bulk gnetization of Co and Ni. K_1 and K_2 are estimated by fitting the normalized M-H loop to a constrained polynomial function ($y = a_1 x + a_3 x^3$) in the range $-0.95M_S < M < 0.95M_S$ (see Fig. 3). Figure 4 shows the separate contributions $K_1 D$ and $K_2 D$ to the effective anisotropy and straight lines obtained by a least-squares fit to data points. As expected, K_1 becomes dominant with increasing Co thickness. We obtain the critical thickness ($t_c^{\mathrm{PMA,Co}}$) of Co in this system when $K_1 D = 0$ and K_V^{Co} is determined by the slope of the straight line. The intercept with the vertical axis gives $2K_S^* = 0.83 \pm 0.099$ erg/cm^2 $= 0.83 \pm 0.099$ mJ/m^2 for this system, which should depend on t^{Ni} [see Eq. (2)]. The critical thickness $t_c^{\mathrm{PMA,Co}} = 6.15 \pm 1.25$ Å of this system is larger and

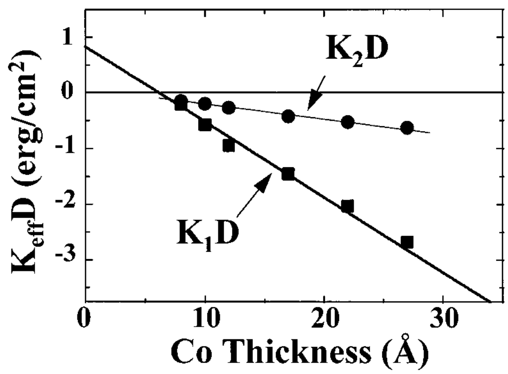

FIG. 4. The product of effective anisotropy constant (K_{eff}) and total magnetic layer thickness D, plotted as a function of Co thickness. From the least-squares fit (straight line) to the data points of K_1D, $2K_S^*(=0.83\pm0.099\ \mathrm{erg/cm^2})$, $K_V^{Co}[=-(1.35\pm0.095)\times10^7\ \mathrm{erg/cm^3}]$, and $t_c^{PMA,Co}(=6.15\pm1.25\ \text{Å})$ have been determined.

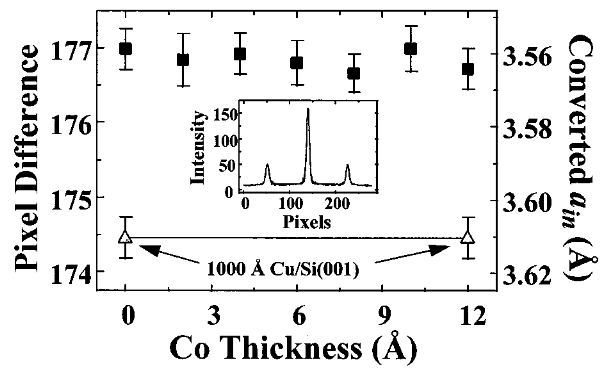

FIG. 5. Pixel difference measured by RHEED (left axis) and converted in-plane lattice parameter (a_{in}, right axis) vs Co thickness. The a_{in} of Cu film at 1000 Å is assumed to be a_{in} of bulk Cu. The inset shows the intensity profile of a 1000 Å Cu/Si and a result of curve fitting to it.

$K_V^{Co}=-(13.5\pm0.95)\times10^6\ \mathrm{erg/cm^3}=-1.35\pm0.095\ \mathrm{MJ/m^3}$ is much smaller than the corresponding values for the Ni/Co/Ni/Cu(001) system.[9] In particular our value for K_V^{Co} is the same as that of the shape anisotropy ($-1.27\ \mathrm{MJ/m^3}$) within experimental error, which is consistent with the result of the work of Krams *et al.* on single crystal Co/Cu(001) films.[13] Polarized neutron reflection magnetometry measurements on a similar structure [Cu/22 Å Co/11 Å Cu/53 Å Ni/Cu/Si(001)] yield 94% of the bulk magnetization for Co,[14] suggesting that the Co film is likely to have a magnetization close to the bulk value in the structure investigated here.

The difference in strain within the Co film between our system and Ni/Co/Ni/Cu(001) (Ref. 9) not only explains the different values for K_V^{Co} but also suggests a way of controlling the critical thickness for PMA in this system. The Ni/Cu(001) structures without Co layers in both systems show PMA. Johnson *et al.*[9] limited the Ni thickness below the critical thickness in order to maintain coherent growth for both Ni and Ni/Co/Ni on Cu(001). Therefore K_V^{Co} of their Co film has two main contributions (shape anisotropy +magnetoelastic anisotropy). But our value of K_V^{Co} suggests that the overlying epitaxial Co films in our system do not experience any strain within experimental error although there is a difference in the ideal lattice constant between fcc Co and fcc Ni. In order to confirm the absence of strain, leading to a vanishing magnetoelastic anisotropy contribution in the Co films, we determined the in-plane lattice parameters (a_{in}) from the streaks in the RHEED images through a line-shape analysis. Figure 5 shows the results of this analysis, in which the left axis represents the directly measured pixel difference of the right and left peaks in the inset and the right axis is a real space value. The inset shows the RHEED intensity profile for a 1000 Å Cu/Si(001) structure and its fitted curve. We have used 4 Gaussian functions for fitting. We can see a clear difference in a_{in} between Cu and Ni but no difference between Ni and Co. The fact that the same value of a_{in} was measured for Ni and Co can be interpreted in two ways. The first is the coherent growth of a Co film on the Ni/Cu(001) structure within the Co thickness range measured by RHEED. The second is that a_{in} of the 60 Å Ni film is the same as a_{in} of the ideal fcc Co, so no further changes in a_{in} are observed. This second view is directly confirmed within experimental error if we convert the measured pixel differences into real space values by assuming that the a_{in} of 1000 Å Cu is the ideal bulk value (3.61 Å) (right axis of Fig. 5). The converted a_{in} of Ni and Co is 3.56 Å which is the lattice constant of an fcc Co structure. The results of our RHEED analysis are also strongly supported by the strain relaxation argument for the incoherent film growth region. In the incoherent growth region, the residual strain ϵ can be expressed as $\epsilon=\eta t_c/t$, where η is the lattice misfit and t_c is the critical thickness of coherent growth.[15] After 60 Å Ni growth on a Cu single crystal, the a_{in} of Ni reaches the value of 3.54 Å if 14 Å (Ref. 16) is assumed as t_c, which is the ideal value within 0.5%. We also found in our earlier work[17] that the a_{in} of an epitaxial 60-Å-Ni film on 600 Å Cu/Si(001) is 3.55 ± 0.010 Å. Therefore we conclude that the Co films on 60 Å Ni do not experience any strain within experimental error and the measured value of K_V^{Co} can be explained in this way.

In conclusion, we have studied the transition from perpendicular to in-plane magnetization in the epitaxial Co/60 Å Ni/Cu(001) system. The value of K_V^{Co}, which comes entirely from the shape anisotropy contribution, is explained by the absence of strain in the Co film as evidenced by our RHEED studies. Our study suggests that the critical thickness for PMA in this system can be controlled via strain in the film.

This work was partly supported by the ESPRIT program of the EC (SPIDER) and EPSRC (UK).

[1] U. Gradmann, J. Magn. Magn. Mater. **54-57**, 733 (1986).
[2] L. Néel, J. Phys. Radium **15**, 225 (1954).
[3] N. C. Koon, B. T. Jonker, F. A. Volkening, J. J. Krebs, and G. A. Prinz, Phys. Rev. Lett. **59**, 2463 (1987).
[4] C. Liu, E. R. Moog, and S. D. Bader, Phys. Rev. Lett. **60**, 2422 (1988).
[5] F. J. A. den Broeder, D. Kuiper, H. C. Donkersloot, and W. Hoving, Appl. Phys. A **49**, 507 (1989).
[6] F. J. A. den Broeder, W. Hoving, and P. J. H. Bloemen, J. Magn. Magn. Mater. **93**, 562 (1991).
[7] G. H. O. Daalderop, P. J. Kelly, and F. J. A. den Broeder, Phys. Rev. Lett. **68**, 682 (1992).
[8] W. L. O'Brien and B. P. Tonner, Phys. Rev. B **52**, 15 332 (1995).
[9] M. T. Johnson, J. J. de Vries, N. W. E. McGee, J. aan de Stegge, and F. J. A. den Broeder, Phys. Rev. Lett. **69**, 3575 (1992).
[10] R. Naik, C. Kota, J. S. Payson, and G. L. Dunifer, Phys. Rev. B **48**, 1008 (1993).
[11] O. Heckmann, H. Magnan, P. le Fevre, D. Chandesris, and J. J. Rehr, Surf. Sci. **312**, 62 (1994).
[12] Chin-An Chang, J. Appl. Phys. **68**, 4873 (1990); G. Bochi, H. J. Hug, D. I. Paul, B. Stiefel, A. Moser, I. Parashikov, H.-J. Güntherodt, and R. C. O'Handley, Phys. Rev. Lett. **75**, 1839 (1995).
[13] P. Krams, F. Lauks, R. L. Stamps, B. Hillebrands, and G. Güntherodt, Phys. Rev. Lett. **69**, 3674 (1992).
[14] G. Lauhoff *et al.* (unpublished).
[15] C. Chappert and P. Bruno, J. Appl. Phys. **64**, 5736 (1988).
[16] S. A. Chambers, H. W. Chen, I. M. Vitomirov, S. B. Anderson, and J. H. Weaver, Phys. Rev. B **33**, 8810 (1986).
[17] Jaeyong Lee, G. Lauhoff, M. Tselepi, S. Hope, P. Rosenbusch, J. A. C. Bland, H. A. Dürr, G. van der Laan, Ph. Schillé, and J. A. D. Matthew, Phys. Rev. B **55**, 15 103 (1997).